

# Visual Quality Control in Heat Shrink Tubing

A. Barth<sup>1,2</sup>, R. Herpers<sup>1,3</sup>, and M. Greßnich<sup>2</sup>

<sup>1</sup> Department of Computer Science, Bonn-Rhein-Sieg University of Applied Sciences,  
Grantham-Allee 20, 53757 Sankt Augustin

<sup>2</sup> DSG-Canusa GmbH & Co. KG, Heidestraße 5, 53340 Meckenheim

<sup>3</sup> Department of Computer Science and Engineering, York University, Toronto,  
Ontario, M3J 1P3, Canada

**Abstract.** In this contribution a machine vision inspection system is presented which is designed as a length measuring sensor. It is developed to be applied to a range of heat shrink tubes, varying in length, diameter and color. The challenges of this task were the precision and accuracy demands as well as the real-time applicability of the entire approach since it should be realized in regular industrial line production. In production, heat shrink tubes are cut to specific sizes from a continuous tube.

A multi-measurement strategy has been developed, which measures each individual tube segment several times with sub pixel accuracy while being in the visual field. The developed approach allows for a contact-free and fully automatic control of 100% of produced heat shrink tubes according to the given requirements with a measuring precision of 0.1mm. Depending on the color, length and diameter of the tubes considered, a true positive rate of 99.99% to 100% has been reached at a true negative rate of > 99.7.

## 1 Introduction

Heat shrink tubing is widely used in electrical and mechanical applications for insulating and protecting cable splices. Especially in the automotive supply industry accuracy demands are very high and quality assurance is an important factor in establishing and maintaining customer relationships [1]. In production, heat shrink tubes are cut into lengths from a continuous tube. During this process, however, deviations from the target length can occur. Any deviations above a tolerable level must be detected. The tubes considered in this application can be black or *transparent* in color. Transparent tubes are translucent and appear slightly yellowish due to a film of hot melt adhesive inside the tube. The tube length ranges from 20mm to 100mm, while the outer diameter varies between 6mm and 12mm. The tolerances are  $\pm 0.5$ mm for a tube length of 20 – 30mm,  $\pm 0.7$  for 31 – 50mm and  $\pm 1.0$ mm for 51 – 100. The measurements have to be accomplished at line production on a conveyor belt in real-time.

The quality control system developed here is designed to reach a control of 100% of produced heat shrink tubes without reducing production velocity. Currently, the conveyor runs at approximately 25m/min, i.e. 250-1250 tubes per minute are cut depending on their size.



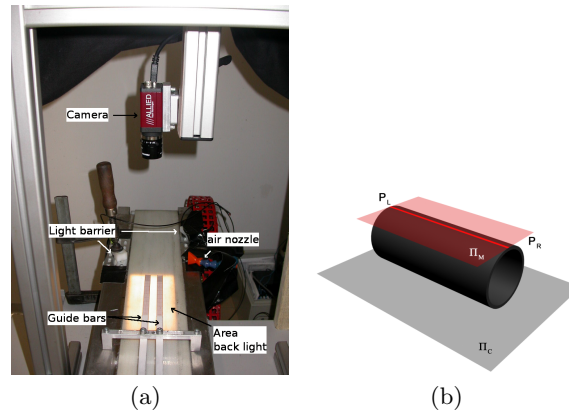


**Fig. 1.** Hardware configuration including camera, area back light, guide bars, and the blow out mechanism (a), Definition of the measuring points in the measuring plane  $\Pi_M$  above the conveyor plane  $\Pi_C$  (b).

## 2 Hardware Configuration

The video camera system is placed at a static position and viewing angle perpendicular to the measuring area of the conveyor belt (see Fig. 1(a)). It is equipped with a standard fix-focal lens of  $16\text{mm}$  focal length. Two guide-bars applied to the conveyor belt guarantee a constant orientation of the tubes. To save computation time the available video image size is reduced to a total image size of  $780 \times 160$  pixel since just this horizontal image strip is carrying the necessary information. The maximum frame rate reached using this resolution is 55 frames per second.

The camera system is calibrated appropriately [2] and a fiber optical area back light is applied to illuminate the measuring area from below through the translucent conveyor belt. This illumination setup allows for shadow free illumination of the objects of interest, which is important for accurate dimensional measuring tasks. The blow out mechanism is placed behind the measuring area including a light barrier, an air nozzle, and a controller unit. On top of the machine vision tasks the control of all additional system components was part of this project.

## 3 Length Measuring Approach

The basic system design concept is a *multi-measurement strategy*, i.e. each tube is measured as often as possible while it is in the visual field of the camera. The total length is computed by averaging over several measurements to yield more robust results. The camera is operated in continuous mode, i.e. no external trigger is required. Fast profile analysis algorithms and model knowledge are used to evaluate whether a tube is completely visible in the image denoted as *measurable*. In addition, the system must be able to track a tube while it is in the visual field to assign measurements to this particular tube. Accurate length measurements of tubes require an accurate detection of the tube edges. A template based tube edge localization method has been developed allowing for

reliable, sub pixel accurate detection results even under the presence of tube edge like background clutter. Once there is evidence that a tube has left the visual field of the camera, all corresponding measurements have to be evaluated with respect to the given target length and tolerances. The resulting good/bad decision must be transferred to the blow out controller. Model knowledge with respect to the inspected tubes and to the constrained conditions has been exploited to optimize the overall performance of the system.

### 3.1 Assumptions and Model Knowledge

In this application, the variety of image situations is limited and constrained by the physical setup. A sufficient contrast between the background and the objects is assumed, as well as a visible spacing between consecutive tubes. The measuring points are defined as the points on tube edges which are closest to the camera (see Fig. 1(b)). Due to perspective tube edges appear convex in the image with the most outer point of an edge corresponding to the left and right measuring point  $p_L$  and  $p_R$  respectively. The visual field of the camera is adapted to the camera distance such as the length of the measuring area in the conveyor plane  $\Pi_C$  is about twice as long as the target tube length (only one tube length is cut over a period of time on one machine). The camera is positioned to yield a *fronto-orthogonal* view [3], i.e. the image plane is parallel to the measuring plane  $\Pi_M$  and  $\Pi_C$ . A consistent characteristic of transparent tubes under back light are two dark stripes at the top and bottom (see Fig. 2(a)) since less light can pass through the tube there.

### 3.2 Profile Analysis

A fast tube localization is reached by the analysis of the average gray level profile of a set of horizontal scanlines equally distributed over the image. Strong peaks of the first derivative of the gray value profile indicate potential tube edges. Segments between such peaks are classified into foreground and background based on the mean intensity of the whole image and the median of each segment (see Figs. 2(a) and 2(b)). If the median gray level of a segment is darker than the overall mean, this segment is assumed to be foreground, and background otherwise. This heuristic turned out to be stable as long as the translucency of the conveyor belt is approximately homogeneous. An extension of the foreground/background classification that is able to handle even non-uniform background situations (e.g. due to dirt on the conveyor belt) is proposed in [4]. Considering the assumptions made in Sec. 3.1 regarding the visual field of the camera, there must be exactly one foreground segment surrounded by two background segments, otherwise measuring is not possible in this particular image. The boundaries of the background surrounded foreground segment can be used to estimate the potential tube edge locations.

### 3.3 Measuring Point Detection

The profile analysis predicts the location of the measuring points very fast, but not precise enough for measuring due to several smoothing and sub-sampling operations that increase the performance [4]. The exact location has to be detected within a certain region of interest (ROI) around the assumed tube ends.



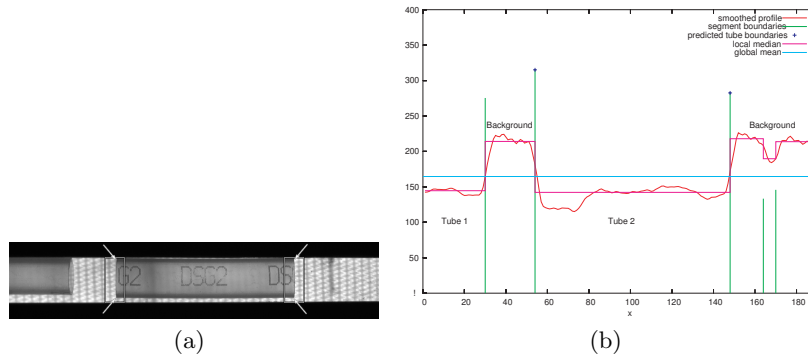


**Fig. 2.** (a) Example image of a heat shrink tube to be analysed. One transparent tube is entirely visible in the visual field of the camera and one is entering from the left. In a profile analysis step, local ROIs around the potential tube edges are computed. Transparent tubes show a varying contrast under back light due to the amount of light that is transmitted. The arrows point onto characteristic strong contrast regions at the upper and lower horizontal tube edges. (b) Profile analysis results of the test image shown in Fig. 2(a)

Therefore, edges of vertical orientation are enhanced using a classical SOBEL operator [5]. Considering the illumination setup and the conveyor belt used, the texture of the belt fabrics is still visible in the image. It may also cause vertical edge responses (see Fig. 3(a)) that might be even stronger than transparent tube edges in worst-case. To yield a semantic interpretation of the tube edges, thresholding or non maximum suppression techniques as used in [6] turned out to be not robust enough and fail if the tube edge contrast is poor. Thus, tube edge specific templates have been developed that allow for distinguishing between background and tube edges by exploiting model knowledge. A template can be computed as

$$T_{\psi}(x, y) = a \exp \left( b \left( \frac{y}{H_T} \right)^2 - \frac{(x - (\psi y/2))^2}{2\sigma^2} \right) \quad (1)$$

It is based on a Gaussian function with standard deviation  $\sigma$  in  $x$ -direction extended with respect to  $y$ . The curvature is denoted by  $\psi$ . A value of  $\psi = 0$  represents no curvature, while the curvature increases (due to the perspective) with increasing values of  $\psi$  ( $\psi \leq 1$ ). The first summand in the exponent of the exponential function is used to emphasize the ends of the template in  $y$ -direction which is motivated by the characteristic response of transparent tubes. The edge detector results in higher values at the corners than at the center,  $b$  controls the amount of height displacement. If  $b$  is set to 0, the template is equally weighted.  $H_T$  represents the template height.  $a$  controls the sign of the template values. For bright-dark edges like at the left boundary, the edge response is assumed negative, thus  $a = -1$ . On the other hand, on the right side  $a = 1$  is taken to model the positive response of dark-bright edges.

Fig. 3(b) shows an example of a template for a slightly curved right tube edge (note the differently scaled axis compared to (a)). A set of  $N$  templates is precomputed for each side between the minimum curvature ( $\psi = 0$ ) and

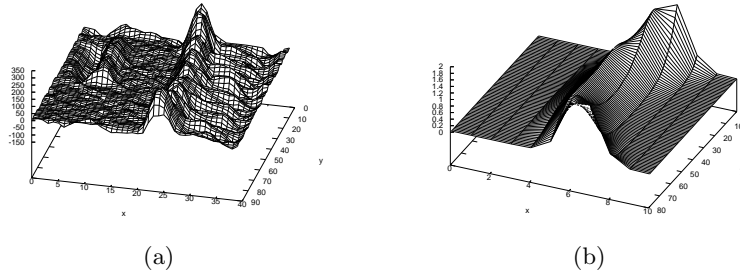


**Fig. 3.** (a) Edge response of a SOBEL operator (right tube end). (b) Example template ( $\sigma = 0.8$ ,  $\psi = 0.001$ ,  $a = 1$ ,  $b = 3$ ). The measuring point is defined at the template's center.

the maximum expected curvature, which has been determined empirically as  $\psi = 0.005$ . In addition, slightly rotated versions of each template ( $\pm 2$  degrees in both directions) are generated as well to cover also tubes that are not ideally horizontal oriented due to a remaining spacing between tubes and guide-bars in order to prevent a blockage. Since cross-correlation is a computationally expensive operation, the template matching can become a bottleneck with larger  $N$ . Thus, applying model knowledge about the expected states, the number of curvatures to be evaluated can be minimized since certain orientations can be excluded depending on the  $x$ -position of the ROI (maximum curvature appears at the boundaries, minimum curvature at the center)[4].

The position where the correlation score maximizes directly relates to the location of the measuring point since it lies exactly in the template center. This location has pixel-grid precision. To reach a higher measuring precision, a continuous function of the correlation results is approximated within a local  $7 \times 1$  neighborhood around the discrete position in  $x$ -direction using cubic splines [7]. This allows for a sub pixel accurate localization of the measuring points.

The tube length in pixels  $l(x)$  at position  $x$  is computed using the Euclidean distance between the left and right measuring point.

Due to perspective, a tube appears larger at the image center than toward the image boundaries as shown in Fig. 4(a). To approximate the ideal case, a perspective correction has been applied to the real measurements. This can be expressed mathematically as:

$$l_{cor}(x) = l(x) + f_{cor}(x) \quad (2)$$

where  $l_{cor}$  is the perspective corrected pixel length, and  $f_{cor}$  a correction function. The perspective variation in the measurements can be approximated by a 2nd order polynomial of the form:

$$f(x) = c_1x^2 + c_2x + c_3 \quad (3)$$

where the coefficients of the polynomial  $c_i$  have to be determined in a teach-in step by fitting the function  $f(x)$  to measured length values  $l(x)$  in least-squares sense. Then, the correction function  $f_{cor}$  can be computed as:

$$f_{cor}(x) = -(c_1x^2 + c_2x) + c_1s^2 + c_2s \quad (4)$$

where  $s$  is the  $x$ -coordinate of the peak of  $f(x)$  with  $s = -c_2/(2c_1)$ , i.e. the point where the first-derivative of  $f(x)$  is zero. Thus,  $f_{cor}$  is the  $180^\circ$  rotated version of  $f(x)$  which is shifted so that  $f_{cor}(s) = 0$ . This function applied to the measurements has the effect that all values are adjusted to approximately one length  $l(s)$ . The corrected length values  $l_{cor}(x)$  are shown in Figure 4(c). The mean value of all measurements represents the true value much better after the perspective correction step. To reduce the computational load the correction function is computed only once for each position at discrete steps and stored in a look up table for faster access.

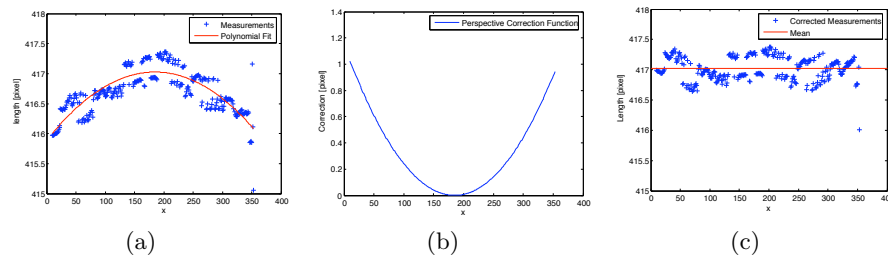


**Fig. 4.** Perspective correction step. (a) The measured length varies depending on the image position in terms of the left measuring point. Due to perspective the length of one tube appears larger at the image center than at the image boundaries. The effect of perspective can be approximated by a 2nd order polynomial. The correction function computed from the polynomial coefficients. (c) Result of the perspective correction.

The perspectively corrected pixel length values of a set of single measurements are averaged to yield the total pixel length  $l_{total}$ . With the assumptions made in Sec. 3.1 regarding the camera position and with a weak-perspective camera model [8] a constant scale factor  $f_{pix2mm}$  can be used to relate a pixel length  $l_{total}$  of tube  $i$  into a real world length  $L_{total}$  as follows:

$$L_{total}(i) = l_{total}(i) f_{pix2mm} \quad (5)$$

This scale factor has to be adapted to the ground truth data during a teach-in step. Therefore, a metallic reference tube of precisely known length and the same diameter as the heat shrink tubes of interest is analysed. The known reference length and the measured length are considered to compute the optimal calibration factor  $f_{pix2mm}$  that results in the smallest error in least-squares sense. To compute the average of all the individual per tube measurements to obtain the total length, a simple tracking heuristic is applied. Firstly it exploits the fact that a tube cannot move against the conveyor moving direction. Again, the  $x$ -coordinate of the left measuring point  $x_{pL}$  is taken as reference. Hence considering the image content assumption, the tube measured at time  $t - 1$  has left the visual field if  $x_{pL}(t) < x_{pL}(t - 1)$ . If no new tube arrives for more than  $\Delta t$  frames, it is also assumed that the previously measured tube has passed the measuring area. In practice,  $\Delta t$  should be chosen by the average number of per tube measurements and the distance between measuring area and light barrier.

The total length is evaluated with respect to the given tolerances. Each tube would be blown out by the system by default. However, if a tube does meet the tolerances, a signal is sent to the blow out controller to let the particular tube pass.

## 4 Results and Evaluation

Several scenarios and experiments have been computed to evaluate the machine vision inspection system. Human ground truth measurements have been used as reference measurement to evaluate the system approach with respect to accuracy and precision.

### 4.1 Evaluation Criteria

The quantitative evaluation criteria include the detection rate  $\Omega_{total}$ , the number of per tube measurements  $\Omega_{PTM}$ , the false positive rate  $\Omega_{FP}$  and the false negative rate  $\Omega_{FN}$ . A detection rate  $\Omega_{total} < 1$  indicates that tubes could pass the visual field of the camera without being measured. Qualitative evaluation criteria are the average standard deviation of the single measurements per tube  $\bar{\sigma}_{tube}$  and the root mean square error  $RMSE$  of  $N$  tubes with respect to manually acquired ground truth measurements:

$$RMSE = \sqrt{\frac{1}{N} \sum_{i=1}^N (L_{total}(i) - L_{gt}(i))^2} \quad (6)$$

where  $L_{total}(i)$  is the computed total length in *mm* of tube  $i$  and  $L_{gt}(i)$  the corresponding ground truth length. Ground truth data has been obtained by manual measurements although there are significant deviation in human measurements observable, since heat shrink tubes are flexible.

### 4.2 Experimental Results

*Repeatability* The measuring precision is related to the repeatability of measurements. In this scenario a few numbers of tubes of known length pass the measuring area 100 times each. The standard deviation of these measurements is an indicator for the precision. For black tubes of 50mm length and 8mm diameter moved at a conveyor velocity of 30m/min a standard deviation of  $\sigma = 0.061$  has been calculated, for transparent tubes of the same size and velocity  $\sigma = 0.051$ . Although transparent tubes are more difficult to detect they have the advantage of being less flexible compared to black tubes. Any deformations of the cross-section have a measurable influence due to perspective distortions. Experiments with an ideal round metallic tube have shown that a much higher precision is possible with  $\sigma = 0.033$  if deformations can be excluded.

*Conveyor Velocity* In this scenario, hundreds of disjunct tubes of 50mm length and 8mm diameter have been inspected at varying conveyor velocities. The results are summarized in Table 1. It has been shown that for black tubes the accuracy of the measurements does not decrease with faster velocities nor with a decreasing number of per tube measurements  $\Omega_{PTM}$  indicated by the  $RMSE$ . Transparent tubes, however, show an increased  $RMSE$  and per tube standard



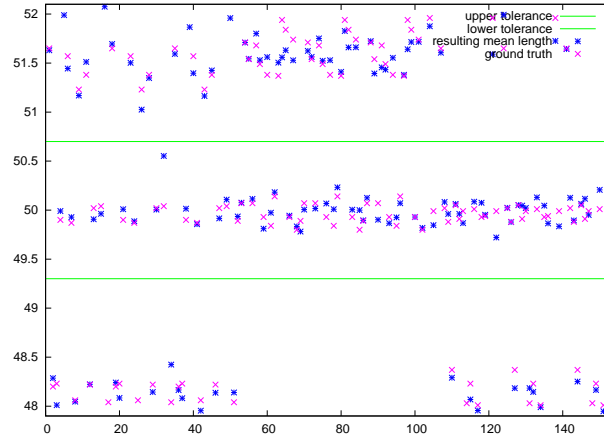


**Fig. 5.** Results of an outlier experiment. The two horizontal lines (green) show the upper and lower tolerance limits. The vision based measurements are marked by stars '\*' (blue) while the associated reference measurements/ground truth by 'x' (pink). 150 transparent tubes of known length (target length 50mm, 8mm diameter, conveyor velocity 30m/min) have been tested. About one third have met the tolerances while two third were manipulated (either too large or too short). All tubes were classified correctly. No false positives and false negatives have been detected.

deviation  $\bar{\sigma}_{tube}$  for higher velocities. The main difference between black and transparent tubes is the detection ratio. While 100% of all black tubes have been detected and measured correctly by the system, some transparent tubes could pass the visual field without being detected at all. This probability increases with faster velocities, since less frames are available to be considered per tube. Transparent tubes may not be detected by the system if the contrast between tube and conveyor belt background is getting poor. Too bright or too dark regions on the conveyor belt (e.g. due to dirt or non-homogeneous material properties) can be sources of such problems.

(a) black					(b) transparent				
$v$ [m/min]	$\Omega_{total}$	$\Omega_{PTM}$	$\bar{\sigma}_{tube}$	$RMSE$	$v$ [m/min]	$\Omega_{total}$	$\Omega_{PTM}$	$\bar{\sigma}_{tube}$	$RMSE$
10	1	11.4	0.05	0.07	10	0.99	9.6	0.06	0.13
20	1	6.9	0.04	0.07	20	0.98	5.2	0.09	0.11
30	1	4.6	0.05	0.07	30	1	3.9	0.15	0.20
40	1	3.2	0.07	0.09	40	0.97	2.4	0.18	0.28

**Table 1.** Evaluation results at different conveyor velocities  $v$  for black and transparent tubes (50mm length, diameter 8mm)

*Tube Diameter* The tube diameter determines the position of the measuring plane  $\Pi_M$ . Accordingly, for maximum precision the calibration factor  $f_{pix2mm}$  has to be adapted if a different tube diameter is processed. The results of hundreds of measurements of 50mm length tubes with diameters of 6, 8, and 12mm moved at conveyor velocities of 30m/min are shown in Table 2. Measurements of black tubes tend to result in a higher  $RMSE$  values for 6 and 12mm diameters



tubes while  $\Omega_{total}$ ,  $\Omega_{PTM}$ , and  $\bar{\sigma}_{tube}$  are almost constant. The increasing error can be explained by two different reasons. Thin 6mm tubes tend to bend along the longitudinal axis. The measured distance in the image does not correspond to the *straight length* of a tube in this case and the tubes are measured shorter. Tubes with a larger diameter are less sensitive to bending. However, 12mm tubes show an increasing amount of elliptical deformations of the cross-section leading to the effect that the measuring points might not lie in the assumed and calibrated measuring plane. Due to perspective, the tubes can be measured longer or shorter.

(a) black					(b) transparent				
Diameter	$\Omega_{total}$	$\Omega_{PTM}$	$\bar{\sigma}_{tube}$	$RMSE$	Diameter	$\Omega_{total}$	$\Omega_{PTM}$	$\bar{\sigma}_{tube}$	$RMSE$
6mm	1	4.8	0.05	0.18	6mm	0.92	2.8	0.18	0.20
8mm	1	4.6	0.05	0.07	8mm	1	3.9	0.15	0.20
12mm	1	4.6	0.07	0.19	12mm	0.98	3.12	0.24	0.20

**Table 2.** Measuring results of 50mm length tubes with different diameter at a velocity of 30m/min.

The resulting  $RMSE$  value for transparent tubes does not change between different diameters. Transparent tubes are less flexible and thus less sensitive to deformations. However, the detection ratio of 6mm tubes decreases significantly, since they are more translucent. Without adjusting the light source, the 6mm transparent tubes disappear in the image (overexposure). The opposite effect can occur if the light intensity gets too low, especially if the conveyor belt is dirty at some regions. In both cases the contrast may not be good enough to locate the measuring points.

*Outlier Detection* A set of 22 tubes of 50mm length and 8mm diameter that meet the tolerances is mixed with 30 tubes of manipulated length. The tubes are placed in random order onto the conveyor belt and the system has to identify all tubes not meeting the tolerances at a conveyor velocity of 30m/min (see fig. 5). This experiment has been repeated 22 times to reach a total number of 1144 independent measuring situations. The total detection rate obtained was  $\Omega_{total} = 0.99$ , i.e. 6 tubes out of 1144 could pass the measuring area without being measured at all. Three tubes have been classified wrongly representing a false negative rate of  $\Omega_{FN} = 0.0026$ , i.e. 0.26%. The false positives are more critical. However, only one tube of manipulated length has been inspected, but was not blown out. This corresponds to a false positive rate of  $\Omega_{FP} = 0.0008$  (0.08%).

## 5 Conclusions and Discussions

A prototype for a vision-based heat shrink tube measuring system has been proposed allowing for an 100% online inspection in real-time of produced heat shrink tubes. A multi-measurement approach has been developed in which each decision whether a tube does meet the given tolerances or not is based on 2-11 individual measurements depending on the tube size and conveyor velocity.



This requires video frame rates of  $\geq 50$ fps to be processed in real-time. Fast algorithms, heuristics and model knowledge have been applied to improve the overall performance. The obtained results in particular for black shrink tubes of all sizes have recently demonstrated that they are able to meet industry requirements.

The experimental results have shown, that the system reaches a measuring precision that allows for reliable measurements of tubes with respect to the specified tolerances at conveyor velocities of up to 40m/min. While deformations mostly influence the measuring results of black tubes, the main difficulties with transparent tubes occur if there is non uniform brightness and/or the texture of the background is misleading. A conveyor belt which is equally translucent over the entire analysis process could prevent many problems. The lighting conditions could be adjusted in such a way that a uniform contrast between tubes and the background could be reached.

In addition, the measuring results have other positive side effects. Assuming the computation of the moving average of the last  $N$  measurements, this value could be used to control the production process. This can be in particular useful during teach-in steps of the entire production system. During the production process, deviations of the target length can be identified before the tolerances are exceeded.

The obtained results recommend a wider application of machine vision based inspection systems for quality control tasks of heat shrink tubes after production. Boring and unreliable manual measurements of a small fraction of the production quantity could be replaced by a reliable and precise automated control of 100% of all produced tubes.

#### **Acknowledgments**

We gratefully acknowledge the financial support of the DSG-Canusa GmbH & Co. KG, Meckenheim, Germany. further acknowledge the support of Phillip Wegner and Patrick Schmitz assisting thousands of measurements.

#### **References**

1. Batchelor, B., Waltz, F.: Intelligent Machine Vision. Springer (2001)
2. Heikkila, J., Silven, O.: A four-step camera calibration procedure with implicit image correction. In: Proc. of the IEEE Computer Vision and Pattern Recognition (CVPR). (1997) 1106–1112
3. Hartley, R., Zisserman, A.: Multiple View Geometry in Computer Vision. 2nd edn. Cambridge University Press (2003)
4. Barth, A.: Visual inspection of fast moving heat shrink tubes in real-time. Master's thesis, Bonn-Rhein-Sieg University of Applied Sciences, Grantham-Allee 20, 53757 Sankt Augustin, Germany (2005)
5. Jähne, B.: Digital Image Processing. 6th edn. Springer (2005)
6. Canny, J.: A computational approach to edge detection. IEEE Transactions on Pattern Analysis and Machine Intelligence (PAMI) **8** (1986) 679–698
7. Press, W.H., Teukolsky, S.A., Vetterling, W.T., Flannery, B.P.: Numerical Recipes in C: The Art of Scientific Computing. 2nd edn. Cambridge University Press, Cambridge, UK (1993)
8. Forsyth, D.A., Ponce, J.: Computer Vision - A modern approach. Pearson Education International (2003)

